JOURNAL OF MATERIALS SCIENCE 19 (1984) 745–752

Hot isostatic pressing of Si_3N_4 with Y_2O_3 additions

O. YEHESKEL*, Y. GEFEN*, M. TALIANKER
Department of Materials Engineering, Ben-Gurion University of the Negev, Beer Sheva, Israel

The effect of Y_2O_3 additive on the properties of hot isostatically pressed silicon nitride was studied. The influence of small additions of Y_2O_3 on the densification of silicon nitride was investigated. The density and elastic moduli of the product increase with increasing of the Y_2O_3 additions. The hot isostatically pressed pure silicon nitride consists of α-Si_3N_4, β-Si_3N_4 and Si_2N_2O; phase content of the hot isostatically pressed silicon nitride with 10 wt % Y_2O_3 addition consists of β-Si_3N_4, yttrium silicate and $Y_2Si_3O_3N_4$. The effect of the outgassing of the specimens prior to hot isostatical pressing on the properties of the final material is discussed.

1. Introduction

Silicon nitride is one of the leading ceramic materials with wide applications at elevated temperatures, when high strength and resistance to oxidation, creep and thermal shock are needed. The process of sintering of pure Si_3N_4 is difficult because of the low self-diffusivity of this covalent material [1]. It is well known, however, that the additions of some oxides to powder of pure Si_3N_4 provide the formation of intergranular liquid phase which aids the densification of the silicon nitride during the sintering process. Another way to densify the material is by applying high pressure to the heated silicon nitride power, i.e. hot pressing. Hot pressed silicon nitride with various oxide additives has been extensively studied [2–8]. Gazza [4, 5] was the first to use Y_2O_3 additions in the hot pressing of Si_3N_4. He found that Y_2O_3 additive not only results in dense high-strength specimens of Si_3N_4 but also improves refractory properties of the material. The amount of about 3 wt % of Y_2O_3 was essential for achieving high density of commercial silicon nitride [4], however greater amount of Y_2O_3 were needed to densify Si_3N_4 of higher purity [5].

During the last decade a new process for fabrication of fully dense silicon nitride has been developed. This process which promises to combine the most attractive features of both sintering and isostatic-pressing technologies is called hot isostatic pressing (HIP) [9, 10].

In the HIP process a gas at high pressure acts via a gas impermeable envelope on a powder of the material during its sintering. The gas pressure in HIP-process is typically higher up to an order of magnitude than that used for uniaxial hot pressing in graphite tools. Hot isostatic pressing offers the possibility of high degree densification of material combined with the ability of fabricating intricately shaped parts.

Larker [9] used the HIP of silicon nitride in order to manufacture integrated turbine wheels. Yeh and Sikora [10] consolidated pure Si_3N_4 at 1760° C at a pressure of 276 MPa, thus obtaining 95% of the theoretical density for the material.

The present study was undertaken to investigate the effect of small amounts of Y_2O_3 additive on the properties of the silicon nitride material fabricated by hot isostatic pressing. Actually the studies were performed within a pseudoternary Si_3N_4–SiO_2–Y_2O_3 system for which phase relations obtained at temperatures between 1600 and 1750° C [11] are represented in Fig. 1. Solid circles, corresponding to 0.5, 2, 5 and 10 wt % of

*Also associated with the Nuclear Research Centre – Negev, PO Box 9001, Beer Sheva, Israel.

0022–2461/84 $03.00 + .12

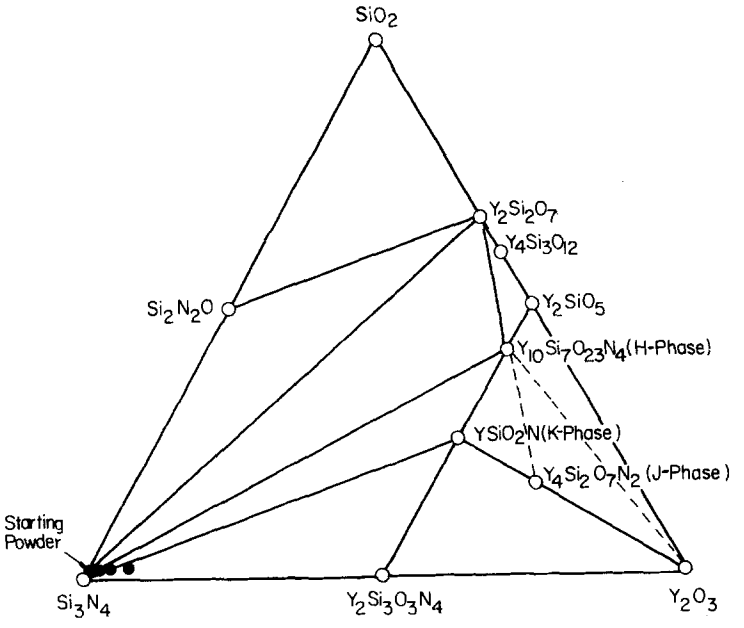

Figure 1 Phase relations in the system Si_3N_4–SiO_2–Y_2O_3 determined from hot pressed specimens at temperatures between 1600 and 1750° C [11].

Y_2O_3, represent the powder compositions examined in our HIP experiments.

2. Experimental procedures

The powder used were high purity silicon nitride* and high purity Y_2O_3† (99.999%). The chemical analysis of metallic impurities in Si_3N_4 was performed by emission spectroscopic method, the oxygen content was determined by gas chromatography in helium carrier gas after fusion in graphite crucible in the presence of platinum, and the Leco apparatus was used to determine the carbon content. The list of impurities in Si_3N_4 is presented in Table I. Traces of free silicon were revealed by X-ray diffractometry.

Mixtures of 0.5, 2, 5 and 10 wt% of Y_2O_3 and Si_3N_4 were blended for 24 h in plastic jars. Powder grinding was not employed in order to avoid further contamination. The mean particle size according to Fisher subsieve sizer was 0.75 μm. The blended mixtures were cold isostatically compacted in rubber bags to 200 MPa. Each compact was machined to about the specimen with diameter of about 13 mm and height of 7 mm. Different specimens were placed into two tantalum canisters which were outgassed during 1 h in vacuum of 6 Pa at 1223 and 823 K, respectively. Then the tantalum canisters were sealed by electron beam welding.

The HIP process was carried out in a laboratory apparatus with a graphite furnace. The HIP regime is given in Fig. 2. The maximum temperature was 2073 ± 20 K and the maximum pressure was 90 MPa. The temperature was measured and controlled by W5Re–W26Re thermocouples, and the pressure was measured with both pressure transducer and a Bourdon type gauge. At the end of the HIP cycle the tantalum canisters were broken and residues were ground on SiC papers.

The density of the specimens was determined by the water immersion method. The water density was determined by a standard weight prior to the measurement of the specimens. In order to avoid water absorption a thin lacquer film‡ was sprayed on the porous specimens. The accuracy of determination of the density was ± 0.3%.

The elastic moduli were determined by ultrasonic measurements. For ultrasonic measurements the faces of the specimens were ground to parallelism that was better than 3 μm. The sound vel-

TABLE I Impurities in the Si_3N_4 (AME) powder (wt%)

Fe	Al	Ca	Mg	Cr	Ti	Mn	Ni	Mo	V	Sn	C	O
0.15	0.05	0.015	0.005	0.05	0.01	< 0.005	< 0.005	0.01	0.01	0.01	0.16	1.75

*Advanced Materials Engineering.
†Research Chemicals.
‡Alfac Products.

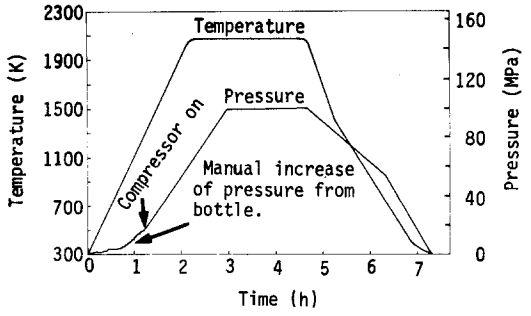

Figure 2 Schematic diagram of the HIP cycle.

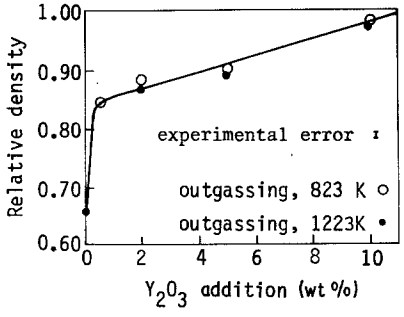

Figure 3 Relative density ρ_s/ρ_m of hot isostatically pressed Si_3N_4 against Y_2O_3 additions. ρ_s is the specimen density and ρ_m is the theoretical density of the mixture.

ocities were measured by the pulse-echo overlap technique [12] using fundamental frequency of 10 MHz. The sound velocities were computed according to the equations:

$$\text{longitudinal velocity, } v_l = \frac{2L}{t_l} \quad (1)$$

$$\text{transverse velocity, } v_t = \frac{2L}{t_t} \quad (2)$$

where t_l and t_t are the elapsed time between the pulse and the echo of longitudinal or transverse waves respectively, and L is the thickness of the specimen. The accuracy of sound velocity measurement was better than 1%.

The elastic moduli were calculated from the following equations:

$$\text{shear modulus, } G = \rho v_t^2 \quad (3)$$

$$\text{Young's modulus, } E = \rho v_t^2 \frac{3v_l^2 - 4v_t^2}{v_l^2 - v_t^2} \quad (4)$$

$$\text{Poisson's ratio, } \nu = \frac{1}{2}\frac{v_l^2 - 2v_t^2}{v_l^2 - v_t^2} \quad (5)$$

$$\text{bulk modulus, } B = \frac{EG}{3(3G - E)}. \quad (6)$$

X-ray diffraction analysis was made using Cu$K\alpha$ radiation. The diffraction patterns for phase identification were run at 1° 2θ min^{-1}.

The specimens for transmission electron microscopy were prepared from the bulk materials using the following technique. Thin slices, about 0.2 mm thick, were cut from the bulk material using a diamond saw. The slices were mechanically ground to a thickness of $\simeq 50\,\mu m$ and then were mounted on a special electron microscope grid with a slot 2 mm x 1 mm. The ion milling apparatus with 5 kV argon ions was used for the final thinning of the specimens. Before examination in the electron microscope JEOL-200B the specimens were coated slightly with the carbon to avoid the charging effect.

3. Results and discussion

3.1. Density

The density of the specimens increased with the increase of amount of Y_2O_3. Such increase was accompanied by changes in the colour of the specimens from light grey to black.

The measured density, ρ_s, and the colour of the specimens are given in Table II. The relative density is defined as ρ_s/ρ_m, where ρ_m is the theoretical density of the mixture of Si_3N_4 and Y_2O_3. The theoretical density of pure Si_3N_4 was taken as 3190 kg m^{-3} and that of pure Y_2O_3 as 5030 kg m^{-3}.

The plot of relative density against Y_2O_3 addition is shown in Fig. 3. It is worth noting the rapid increase in the density of Si_3N_4 doped with 0.5 wt % Y_2O_3, as compared with pure Si_3N_4. Such a density increase of the Si_3N_4 doped with Y_2O_3 appears to be due to the formation of intergranular glass phase. This intergranular phase has been clearly observed in the electron microscope for the specimens with 5 and 10 wt % of Y_2O_3.

The increase in the density of hot isostatically

TABLE II Density (kg m^{-3}) and colour of hot isostatically pressed Si_3N_4

Y_2O_3 addition (wt %)	0	0.5	2	5	10
Outgassing 823 K	–	2726	2850	2928	3282
Outgassing 1223 K	2105		2797	2910	3280
Colour	light grey	grey	dark grey	dark grey	black

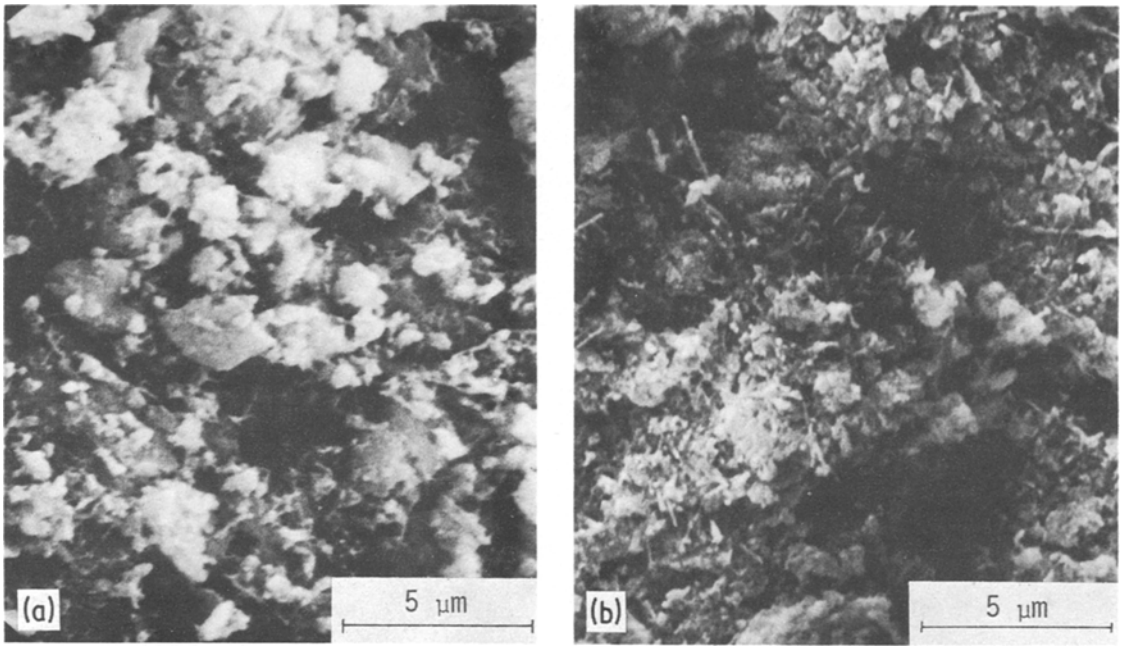

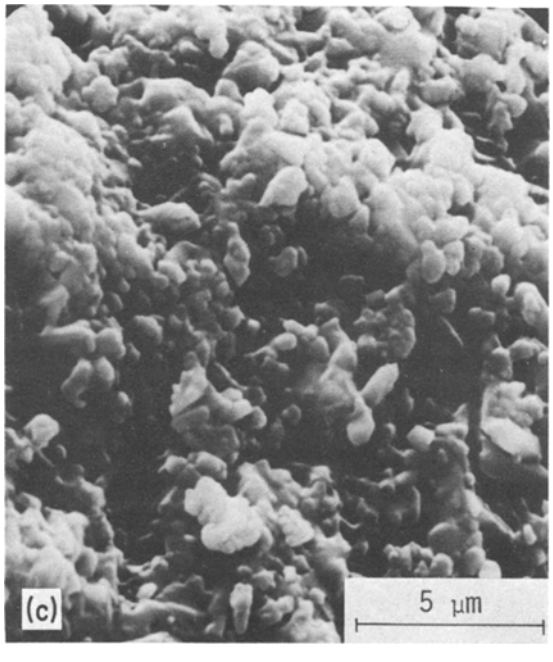

Figure 4 SEM micrographs of the microstructure of the silicon nitride. (a) Starting power, (b) fracture of cold isostatically pressed specimen ($P = 200$ MPa), (c) fracture of hot isostatically pressed Si_3N_4 with 10 wt% Y_2O_3.

pressed material is almost linear with the Y_2O_3 addition. It indicates that the amount of glass phase increases with the amount of additive used. From Fig. 3 it can be seen that approximately 11 wt% Y_2O_3 is needed to densify Si_3N_4 completely. There is no substantial difference in the density of the specimens which were outgassed at two different temperatures, however, the specimens outgassed at the lower temperature exhibit slightly higher densities. It can be explained by suggesting that during the outgassing the impurities partially evaporated. At lower outgassing temperature less evaporation occurred, thus more impurities could contribute to the formation of intergranular liquid phase providing better densification of the specimens. The specimens with 10 wt% Y_2O_3 contained sufficient amount of the glass-forming agent, therefore the effect of outgassing temperature difference became insignificant.

3.2. Microstructure

Figs. 4a to c show the microstructure of the starting powder (Fig. 4a), the fracture of the cold isostatically compacted specimen (Fig. 4b) and the fracture of the hot isostatically pressed Si_3N_4 doped with 10 wt% Y_2O_3 (Fig. 4c). Both in the starting material and in the cold isostatically compacted specimens the particles have sharp edges, while in the hot isostatically pressed specimen the intergranular fracture and rounded edges of the grains are observed. It is assumed that the rounded edges were formed by dissolution of the sharp grain edges in the intergranular liquid phase during the sintering. The intergranular fracture of the hot

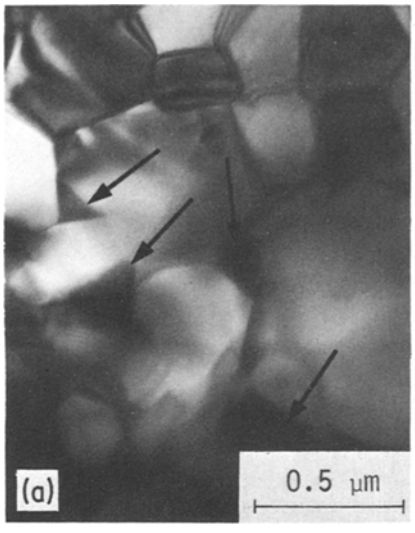

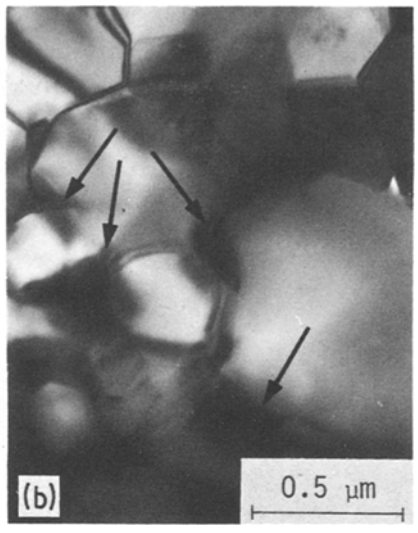

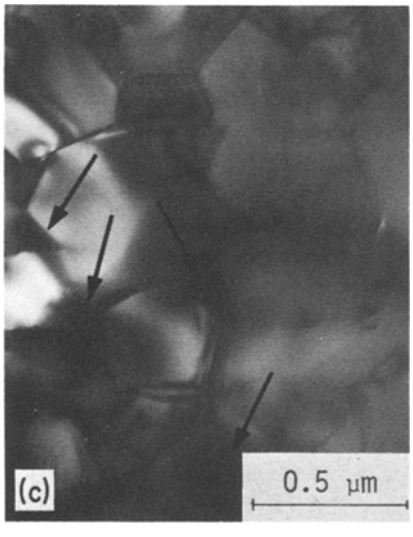

Figure 5 Bright-field transmission electron micrographs showing the same area of the specimen under different diffraction conditions. The regions indicated by arrows are identified as amorphous. The specimen is a hot isostatically pressed Si_3N_4 with 10 wt% Y_2O_3.

isostatically pressed specimen is an indication of a lower adhesion strength between the grains as compared to the strength of the grains. The formation of the liquid phase in the course of sintering results in the appearance of intergranular amorphous solid as was observed by transmission electron microscopy. Those regions of the specimen which show no contrast variation with the specimen tilt were interpreted as amorphous. For example, the transmission electron micrographs in Figs. 5a to c were recorded from the same area of the specimen under different diffraction conditions. The regions in Figs. 5a to c marked by arrows did not reveal a visible change in contrast when the specimen tilt was performed. Such regions of the specimen were identified as amorphous.

3.3. X-ray analysis

The phase content of the starting materials and the hot isostatically pressed specimens were examined by X-ray diffraction. The starting powders consisted of α-Si_3N_4, β-Si_3N_4 and traces of silicon. The relative $\alpha/\alpha+\beta$ content was calculated from the peak heights according to:

$$\frac{\alpha}{\alpha+\beta} = \frac{\alpha(210)+\alpha(210)}{\alpha(201)+\alpha(210)+\beta(101)+\beta(210)} \quad (7)$$

TABLE III Observed and calculated diffraction data of the F-phase in hot isostatically pressed Si_3N_4 + 10 wt% Y_2O_3

h k l	d_{obs} (nm)	d_{cal} (nm)	$(I/I_0)_{obs}$
2 0 0	0.4040	0.4049	27
1 1 1	0.3852	0.3841	19
0 0 2	0.3370	0.3369	22
1 0 2	0.3105	0.3111	32
2 1 0	0.3053	0.3061	39
2 1 1	0.2791	0.2787	100
1 1 2	0.2728	0.2733	37
3 0 0	0.2694	0.2699	34
2 0 2	0.2592	0.2590	27
3 1 1	0.2129	0.2131	12
3 0 2	0.2108	0.2107	19
4 0 0	0.2014	0.2025	25
2 2 2	0.1926	0.1921	50
3 1 2	0.1864	0.1869	22
3 2 1	0.1794	0.1791	17
4 1 0	0.1771	0.1767	25

TABLE IV Lattice parameters of silicon yttrium oxynitride and of yttrium orthosilicate

Chemical Formula	Structure	Lattice parameters		Reference
		a (nm)	c (nm)	
$Y_5(SiO_4)_3N$	Hexagonal	0.941	0.676	[14]
$Y_{10}(SiO_4)_6N_2$	Hexagonal	0.9368	0.6355	[16]
$10Y_2O_3 \cdot 9SiO_2 \cdot Si_3N_4$	Hexagonal	0.9436	0.6822	[17]
$Y_{4.67}(SiO_4)_3O$	Hexagonal	0.9347	0.6727	[18]
Assumed $Y_{4.67}(SiO_4)_3O$	Hexagonal	0.9351	0.6738	Present work

The relative amount of α-phase in the powder of pure Si_3N_4 was ≃ 70%. After hot isostatic pressing of pure Si_3N_4 X-ray analysis revealed the reflections of β-Si_3N_4, α-Si_3N_4 and reflections of silicon oxinitride (Si_2N_2O). The relative amount of α-phase decreased to ≃ 40%. The specimens with 10 wt % Y_2O_3 consisted mainly of β-Si_3N_4. Neither α-Si_3N_4 nor Si_2N_2O could be detected. However, an appreciable amount of an additional phase designated here as F-phase, and traces of $Y_2Si_3O_3N_4$ compound were observed.

The X-ray data (see Table III) related to the F-phase were indexed in terms of a hexagonal cell. A computer program [13] was employed to calculate the lattice parameters of the F-phase which were $a = 0.9351$ nm and $c = 0.6738$ nm, and there was good agreement between the observed and the calculated values. As it can be seen from Table IV the lattice parameters for the F-phase were slightly different from those reported by Jack [14] and Rae *et al.* [15] for the H-phase, which was identified as the N-apatite with the chemical formula $Y_5(SiO_4)_3N$. In other works Gauckler *et al.* [16] reported that the lattice parameters of the apatite $Y_{10}(SiO_4)_5N_2$ were $a = 0.9368$ nm and $c = 0.6355$ nm and Wills *et al.* [17] obtained $a = 0.9436$ nm and $c = 0.6822$ nm for the compound $10Y_2O_3 \cdot 9SiO_2 \cdot Si_3N_4$. In their other study Wills *et al.* [18] oxidized an apatite $Y_5(SiO_4)_3N$ and the product was identified as $Y_{4.67}(SiO_4)_3O$ with the lattice parameters $a = 0.9347$ nm and $c = 0.6727$ nm. The lattice parameters of the F-phase were in best agreement with the latter results of Wills *et al.* [18], therefore the F-phase was identified as yttrium orthosilicate $Y_{4.67}(SiO_4)_3O$.

3.4. Elastic moduli

Figs. 6a and b represent the increase in the elastic moduli of hot isostatically pressed specimens with the addition of Y_2O_3. The graphs in Figs. 6a and b and Fig. 3 look very much alike, but with respect to the same increase in the Y_2O_3 content the elastic moduli increase faster than the density. The plausible explanation of this difference is that the change of the elastic moduli with the addition of Y_2O_3 reflects the increaase of the contact area between the adjacent particles, whilst the density change reflects the decrease in the volume of the pores. With the same increase in Y_2O_3 content (and the consequent increaase of the intergranular amorphous phase) the contact area between the

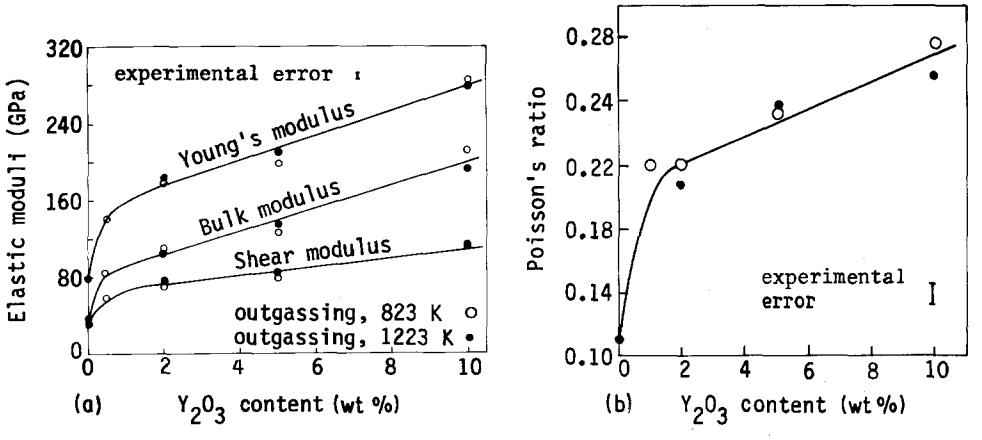

Figure 6 Change of the elastic moduli with Y_2O_3 addition. (a) Young's modulus, shear modulus and bulk modulus. (b) Poisson's ratio.

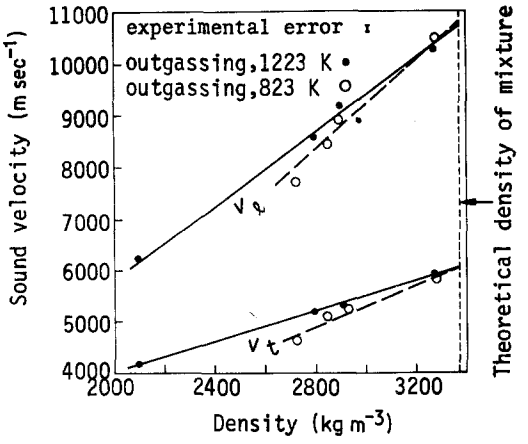

Figure 7 Change of the sound velocities of hot isostatically pressed Si_3N_4 with specimen density.

particles changes faster than the volume of the pores.

It should be noted that in Fig. 6 there is no significant difference in the elastic moduli of the specimens outgassed at different temperatures. On the other hand, the effect of the outgassing temperature on v_l and v_t can be discerned in Fig. 7, where the sound velocities v_l and v_t are given against the specimen density. Three features can be deduced from Fig. 7. The first is the increase of the v_l and v_t with the density, which logically has to be expected. The second is that the sound velocities of the material for which outgassing was carried out at higher temperatures are slightly higher than those for which outgassing was conducted at lower temperature. Such a result can be probably interpreted as an indication that the elastic moduli of the intergranular amorphous phase for these two cases are slightly different. It might be that at higher outgassing temperature less impurities remain, thus leading to the appearance of more refractory and hence more rigid intergranular phase. The third feature is that the difference between sound velocities measured for the same Y_2O_3 content but corresponding to different outgassing temperatures diminishes with the increase of density. Such tendency might also be related to the assumption that the outgassing temperature influences the amount of impurities and hence the rigidity of the amorphous phase. Since the changes in the rigidity due to different outgassing temperatures are minor, their influence upon the sound velocities can be detected only for low Y_2O_3 content. When the Y_2O_3 content increases and thus the amount of amorphous phase is high enough, then the effect of different outgassing temperatures should not be distinguishable, being overwhelmed by the formation of the amorphous phase itself.

Analysis of Figs. 3 and 7 shows that at the proper Y_2O_3 content a complete densification can be achieved by HIP process. It can be calculated that the Young's modulus for completely dense material should be 310 GPa, shear modulus $G =$ 125 GPa, bulk modulus $B = 220$ GPa and the Poisson ratio should be 0.27. The values of the elastic moduli of the hot isostatically pressed silicon nitride are comparable to those of commercial silicon nitride produced by other technologies [19–22] (see Table V).

4. Conclusions

Hot isostatic pressing of silicon nitride doped with Y_2O_3 produces material with density and elastic moduli which are comparable to those of commercial silicon nitride manufactured by other tech-

TABLE V Room temperature elastic moduli of Si_3N_4 fabricated by various techniques as measured by the sonic or the ultrasonic techniques

Density (kg m^{-3})	Additives (wt %) or trade name	E (GPa)	G (GPa)	B (GPa)	ν	Technology	Reference
3281	$10Y_2O_3$	283	111.3	206	0.267	HIP	Present work
2920	$5Y_2O_3$	205	82.5	132	0.238	HIP	Present work
2105	–	79.6	35.7	34.4	0.115	HIP	Present work
3180	Norton	290	118	178	0.220	HP	[21]
3050	Ceradyne	245	101	142	0.215	HP	[21]
2370	Alcan	128	55	63.4	0.170	SC*	[21]
>3100	$8Y_2O_3 + 1MgO$	240	94	179	0.275	HP	[22]
3178	Norton (HS-130)	313	121	252	0.290	HP	[20]
2000	~1 wt % Fe	77	32.3	41.7	0.192	Flow RB†	[19]
2400	~1 wt % Fe	157	63.4	100.2	0.239	Static RB	[19]

*SC = Slip Casting.
†RB = Reaction Bonded.

nologies. The densification by HIP is determined by the amount of Y_2O_3 and approximately 11 wt% Y_2O_3 is needed to densify Si_3N_4 completely, at 2073 K and at 90 MPa. The elastic moduli of the product increase systematically with density, and for completely dense material should reach the following values: $E = 310$ GPa, $G = 125$ GPa, $B = 220$ GPa. The experimentally determined sound velocities depend linearly on the density and display a slight dependence on outgassing temperature.

The hot isostatically pressed silicon nitride with 10 wt% Y_2O_3 additive consists mainly of β-Si_3N_4 with appreciable amount of yttrium orthosilicate $Y_{4.67}(SiO_4)_3O$ and small amounts of $Y_2Si_3O_3N_4$.

Acknowledgements

The authors are grateful to Dr G. Kimmel for computer refining of the X-ray data and to Messrs. D. Kalir, H. Klein and A. Segal for their assistance in the measurements.

References

1. A. J. MOULSON, *J. Mater. Sci.* **14** (1979) 1017.
2. I. C. HUSEBY and G. PETZOW, *Powder Met. Int.* **6** (1974) 17.
3. K. S. MAZDIYASNI and C. M. COOKE, *J. Amer. Ceram. Soc.* **57** (1974) 536.
4. G. E. GAZZA, *ibid.* **56** (1973) 662.
5. *Idem, Amer. Ceram. Soc. Bull.* **54** (1975) 778.
6. A. TZUGE, K. NISHIDA and M. KOMATSU, *J. Amer. Ceram. Soc.* **58** (1975) 323.
7. W. ENGEL, *Powder Met. Int.* **10** (1978) 124.
8. L. J. BOWEN, R. J. WESTON, T. G. CARRUTHERS and R. J. BROOKE, *J. Mater. Sci.* **13** (1978) 1199.
9. H. T. LARKER, AGARD SP-276 P 18-1ff March 1980, available from NTIS.
10. H. C. YEH and P. F. SIKORA, *Amer. Ceram. Soc. Bull.* **58** (1979) 444.
11. F. F. LANGE, S. C. SINGHAL and R. C. KUZNICKI, *J. Amer. Ceram. Soc.* **60** (1977) 249.
12. E. P. PAPADAKIS, *J. Acoust. Soc. Amer.* **42** (1967) 1045.
13. G. KIMMEL, NRCN, private communication.
14. K. H. JACK, *J. Mater. Sci.* **11** (1976) 1135.
15. A. W. J. M. RAE, D. P. THOMPSON, N. J. PIPKIN and K. H. JACK, *Special Ceram.* **6** (1975) 347.
16. L. J. GAUCKLER, H. HOHNKE and T. Y. TIEN, *J. Amer. Ceram. Soc.* **63** (1980) 35.
17. R. R. WILLS, S. HOLMQUIST and J. M. WIMMER, *J. Mater. Sci.* **11** (1976) 1305.
18. R. R. WILLS, J. A. CUNINGHAM, J. M. WINNER and R. W. STEWART, *J. Am. Ceram. Soc.* **59** (1976) 259.
19. R. W. JONES, K. C. PITMAN and M. W. LINDLEY, *J. Mater. Sci.* **12** (1977) 563.
20. J. W. EDINGTON, D. J. ROWCLIFFE and J. HENSHALL, *Powder Met. Int.* 7 (1975) 82.
21. W. A. FATE, *J. Appl. Phys.* **46** (1975) 2375.
22. A. GIACHELLO, P. C. MARTINENGO, G. TOMMASINI and P. POPPER, *Amer. Ceram. Soc. Bull.* **59** (1980) 1212.

Received 11 March
and accepted 24 June 1983